ELSEVIER

Materials Science and Engineering A 449–451 (2007) 1083–1086

MATERIALS SCIENCE & ENGINEERING A

www.elsevier.com/locate/msea

Decomposition of intermetallics during high-energy ball-milling

Y.S. Kwon [a,*], P.P. Choi [a], J.S. Kim [a], D.H. Kwon [a], K.B. Gerasimov [b]

[a] *Research Center for Machine Parts and Materials Processing (ReMM), School of Materials Science and Engineering, University of Ulsan, Ulsan 680-749, Republic of Korea*

[b] *Institute of Solid State Chemistry and Mechanochemistry, Kutateladze 18, Novosibirsk 128, 630128 Russia*

Received 22 August 2005; received in revised form 16 October 2005; accepted 26 February 2006

Abstract

The decomposition behavior of FeSn, CoSn and $CoIn_2$ intermetallics under high-energy ball-milling has been investigated using X-ray diffraction, calorimetric and magnetization measurements. Upon milling a large amount of the FeSn intermetallic decomposes into Fe_5Sn_3 and $FeSn_2$, where the average grain size of the product phases stays nearly constant with milling-time. Similar observations are made for the CoSn intermetallic, which decomposes into Co_3Sn_2 and Sn. It is suggested that the mechanically driven decomposition of FeSn and CoSn results from local melting of powder particles due to high temperature pulses during ball collisions. In contrast to FeSn and CoSn, $CoIn_2$ does not undergo decomposition upon milling. The different decomposition behaviors of the studied intermetallics may be attributed to the volume changes occurring with a decomposition process. Whereas a negative volume change is associated with the decomposition of FeSn and CoSn into their product phases, the decomposition of $CoIn_2$ leads to an increase in volume. Hence, high local stresses under ball collisions are expected to make the mechanically induced decomposition of FeSn and CoSn favorable but rather hinder the decomposition of $CoIn_2$.

Keywords: Intermetallics; Decomposition; Ball-milling

1. Introduction

Mechanically driven decomposition of intermetallics is probably the most inscrutable phenomenon observed for mechanical milling (MM). In some cases milling leads to mixing of initially heterogeneous power blends down to the atomic level with formation of a single solid phase, whereas in other cases demixing of a single solid phase occurs under the same milling conditions. To formulate a predictive model of MM it is useful to elucidate the processes, underlying the mechanically induced decomposition of intermetallics.

Loeff and Bakker were the first to observe the decomposition of intermetallics upon high-energy ball milling [1]. According to their data, some La-based intermetallics decomposed into fcc β-La and other elemental components. However, further studies proved that the fcc phase was not pure lanthanum but LaN [2]. In this case, the decomposition turns up a selective oxidation reaction with nitrogen. Nevertheless, there are other examples of mechanically driven decomposition, which are not due to contamination effects. The decomposition of $Nd_2Fe_{14}B$ and related compounds, first observed by Alonso et al. [3], was reproduced in a number of other studies regarding the synthesis of nanocomposite magnets. Smith and McCormick showed that Sm_2Fe_{17} decomposes during MM into α-Fe and an amorphous phase [4]. Tang et al. [5,6] observed the decomposition of the $NdFe_{11}Ti$ and $Nd_3(Fe,Ti)_{29}$ intermetallics into α-Fe(Ti) and an amorphous phase. Kwon et al. [7] reported the decomposition of Fe_6Ge_5 into $Fe_{2-x}Ge$ and FeGe (B20) and the decomposition of Fe_2Ge_3 into $FeGe_2$ and FeGe (B20). Except for the phases decomposing due to contamination effects all intermetallics which decompose during MM undergo peritectic or peritectoid decomposition upon heating. Kwon et al. [7] ascribed the mechanically driven decomposition of Fe_6Ge_5 and Fe_2Ge_3 intermetallics during MM in a high-energy planetary ball-mill to a local melting process of powder particles due to ball collisions. Their assumption was based on the observation that these two phases decompose almost completely upon MM, although they are favorable in a model of enhanced solid-state diffusion. In this work, some further model systems with peritectic melting points, i.e. FeSn, CoSn and $CoIn_2$, have been studied with respect to their decomposition behavior during high-energy ball-milling. It is the aim of this work

* Corresponding author. Tel.: +82 52 259 2107; fax: +82 52 259 2109.
E-mail address: yskwon@ulsan.ac.kr (Y.S. Kwon).

0921-5093/$ – see front matter © 2006 Elsevier B.V. All rights reserved.
doi:10.1016/j.msea.2006.02.267

to provide evidence in favor of or against the local melting model.

2. Experimental

FeSn, CoSn and $CoIn_2$ intermetallics were prepared by mechanically alloying proper amounts of high purity elemental powders (Fe (99.99%), Co (99.95%), Sn (99.99%) and In (99.999%)) and subsequently homogenizing the alloyed powders of FeSn, CoSn and $CoIn_2$ composition for 10 h under hydrogen atmosphere at 970 K, 1200 K and 800 K, respectively. The obtained intermetallics were milled in a high-energy planetary ball-mill (AGO-2) with a centrifugal acceleration of 226.3 m/s^2 under protective Ar atmosphere. Hardened steel vials and balls were used. The chosen powder to ball weight ratio was 10 g:200 g per vial. Structure and phase composition of the samples were determined by means of X-ray diffraction (XRD), using Co Kα-radiation. In addition, differential scanning calorimetry (DSC) and magnetization measurements in a vibrating sample magnetometer, applying a field of 17.3 kOe at room temperature, were performed.

3. Results and discussion

Fig. 1(a–c) shows the XRD patterns of the initial FeSn intermetallic powder and of powders milled for 20 and 90 min, respectively. It can be recognized that the FeSn phase decomposed under MM into a mixture of $FeSn_2$ and Fe_5Sn_3. The phase compositions of the milled samples were determined from the Rietveld fitting of the diffraction patterns, using the Powder Cell 2.3 program. Thus determined volume fractions of the existing phases amounted to 63% FeSn, 19.3% $FeSn_2$ and 17.7% Fe_5Sn_3 after 20 min MM and 14.7% FeSn, 43.4% $FeSn_2$ and 41.9% Fe_5Sn_3 after 90 min MM. The decomposition degree of FeSn increased with milling time and reached a steady state after prolonged milling, i.e. $t \geq 60$ min. From the parameters of diffraction peak fitting, the average grain size, the size which

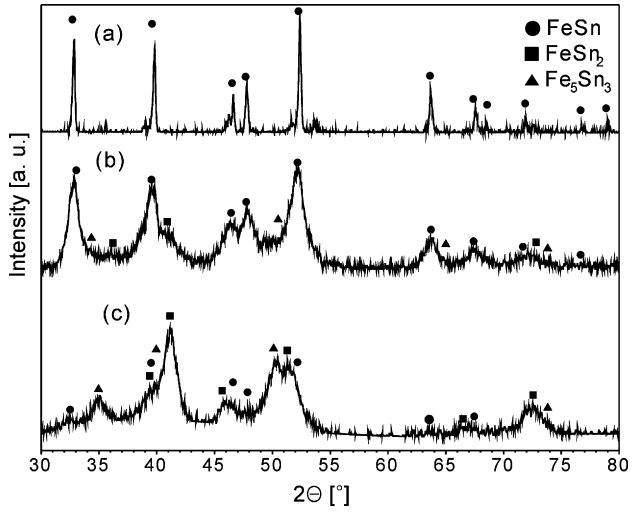

Fig. 1. XRD patterns of the FeSn intermetallic (Co Kα radiation): (a) before MM, (b) after 20 min MM and (c) after 90 min MM.

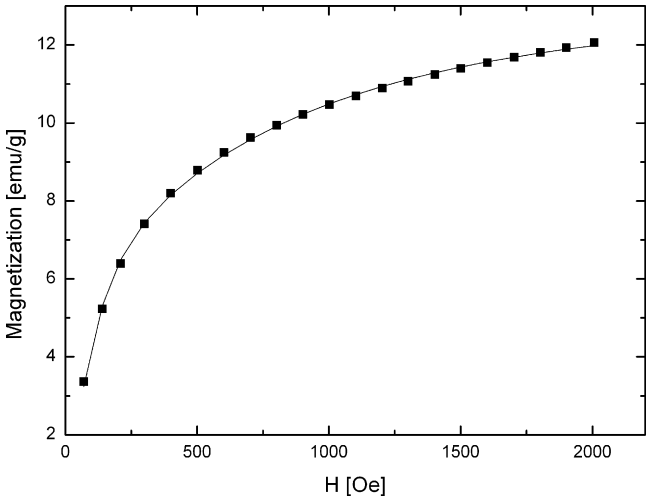

Fig. 2. Room-temperature magnetization curve of milled FeSn intermetallic with a small degree of decomposition. Squares represent experimental data and the solid line is fitting by Eq. (1).

is suitable for coherent X-ray scattering, was determined. The grain sizes were approximately equal to 10 nm for all phases, and changed only slightly with increasing milling time.

All phases in the milled powders must possess superparamagnetic behavior at an adequately high temperature owing to the small grain sizes. The small magnetic moment in antiferromagnetic FeSn and $FeSn_2$ is caused by an incomplete magnetic compensation. Fig. 2 shows a typical room-temperature low-field magnetization curve of a milled FeSn sample with a relatively small amount of decomposition. The magnetization curve shows no hysteresis, i.e. magnetization and demagnetization curves coincide. It is known [8] that anhysteretic magnetization curves can be well described by a superposition of Langevin functions characterized by different values of the magnetic moment. Such a fit allows for the determination of the average magnetic moment in the system as well as of the spread of the magnetic moment distribution. The grain sizes obtained from applying this procedure are consistent with results taken from different magnetic measurements [9] and from structural data analysis [10]. The magnetization curves of FeSn samples with a decomposition degree of less than 60% may well be fitted by a sum of only two Langevin functions (compare Fig. 2):

$$M = N_1 M_1 \left[\coth\left(\frac{M_1 H}{kT}\right) - \frac{kT}{M_1 H}\right] + N_2 M_2 \left[\coth\left(\frac{M_2 H}{kT}\right) - \frac{kT}{M_2 H}\right], \quad (1)$$

where N_1 is the number, M_1 the average magnetic moment of the ferromagnetic (Fe_5Sn_3) grains, N_2 the number, M_2 the average magnetic moment of the antiferromagnetic (FeSn and $FeSn_2$) grains, H the magnetic field, k the Boltzmann constant and T is the absolute temperature. The fit parameter N_1 increased with milling time while the magnetic moment M_1 of the ferromagnetic particles changed only slightly in the range from 6.6×10^{-16} to 9.0×10^{-16} emu for small decomposition degrees of FeSn. The average grain volumes and sizes of the

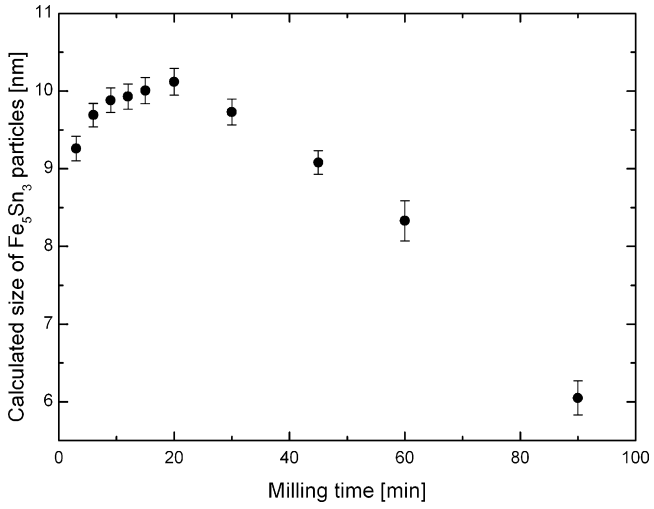

Fig. 3. Estimated grain sizes of Fe_5Sn_3, obtained from fitting the magnetization curve of the FeSn intermetallic to the sum of two Langevin functions, as a function of milling time.

Fe_5Sn_3 phase were estimated from the N_1 values, using 2.10 μ_B for the magnetic moment of the Fe atoms in the Fe_5Sn_3 phase and 8.71 g/cm^3 for the density of this phase [11]. It was assumed that grains have cubic shape. Fig. 3 shows the plot of estimated grain sizes versus the milling time. The grain size remains approximately constant for the first 30 min of MM. The decrease in the estimated grain size with further increase in milling time can be ascribed to the magnetic interaction between the grains in the nanocomposite. In fact, milled powders with a decomposition degree higher than 60% (when milling time exceeded 30 min) showed hysteretic behavior. In this case, the magnetization curves cannot be well fitted by Eq. (1).

Fig. 4(a–c) shows the XRD patterns of the CoSn powder in the initial state and after milling for 30 min and 90 min, respectively. All peaks of the initial powder can be assigned to the CoSn phase. After milling the most intensive reflections ((1 0 1), (1 0 2) and (1 1 0)) of the high-temperature polymorph of Co_3Sn_2 occur, while the intensities of the CoSn reflections decrease. Hence, it can be concluded that the CoSn phase decomposes upon milling into Co_3Sn_2 and a phase with higher Sn content ($CoSn_2$, $CoSn_3$ or Sn(Co)). The latter cannot be identified by means of XRD due to an overlap of its reflections with those stemming from the initial CoSn phase. However, DSC analyses of a milled sample gave evidence in favor of the formation of the Sn(Co) solid solution. The volume fraction of the Co_3Sn_2 phase was determined from Rietveld analyses of the XRD peaks in Fig. 4(b and c) and amounts to 43% and 65% after 30 min and 90 min MM, respectively. The decomposition degree of CoSn was not determined for powders milled for longer milling times, as a significant amount of iron impurities stemming from the balls and vial was detected in such samples. Measuring the broadening of the XRD peaks, the average grain size of the Co_3Sn_2 phase was estimated to be between 15 nm and 17 nm for 30–90 min MM and was therefore found to stay nearly constant. Such a behavior is similar to observations made for the product phases of mechanically driven decomposition of the FeSn intermetallic.

Fig. 5(a and b) shows the XRD patterns of the $CoIn_2$ powder in the initial state and after milling for 90 min, respectively. The XRD pattern of the milled sample does not reveal any additional peaks but only peak broadening. Although $CoIn_2$ has a lower peritectic melting point (T_m = 823 K [12]) than CoSn (T_m = 1209 K [12]) there is no evidence of its decomposition even after prolonged milling. This observation was confirmed by magnetization measurements. If mechanically induced decomposition of $CoIn_2$ occurred, one of the resulting products would be ferromagnetic Co. However, milled powders showed only small magnetization (<1 emu/g) due to iron contamination from the milling tools.

Two explanations for the decomposition of FeSn and CoSn intermetallics are possible. The first is based on the assumption that the local temperature pulses due to ball collisions have a small value, insufficient for local melting. In this case, the decomposition should be accounted for by a change in the relative stabilities of the phases in the Fe–Sn and Co–Sn system

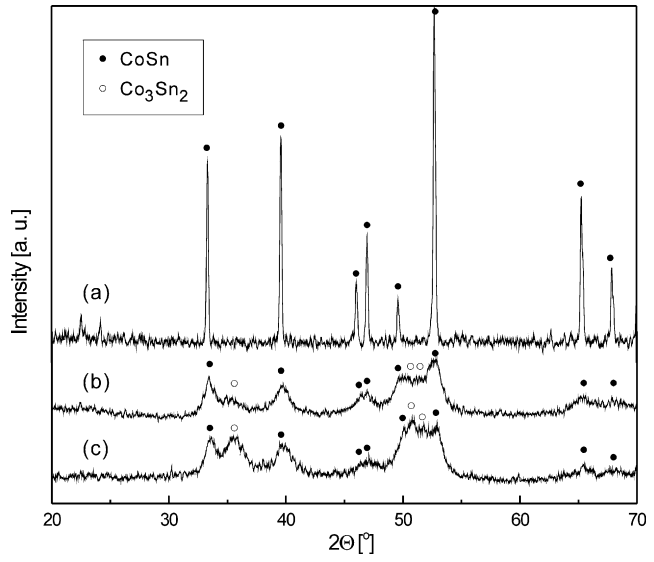

Fig. 4. XRD patterns of the CoSn intermetallic (Co Kα radiation): (a) before MM, (b) after 30 min MM and (c) after 90 min MM.

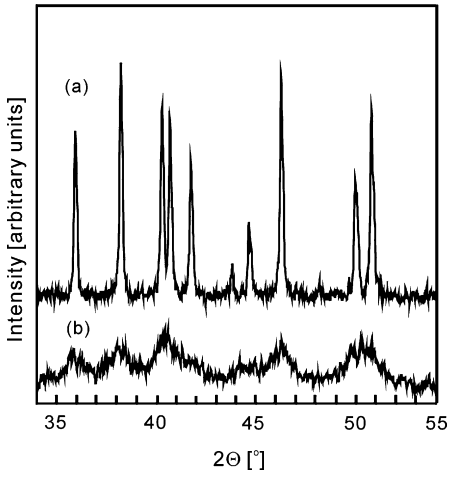

Fig. 5. XRD patterns of the $CoIn_2$ intermetallic (Co Kα radiation): (a) before MM, (b) after 90 min MM.

owing to preferential accumulation of defects in the FeSn and CoSn phases during MM. The decomposition would then occur by solid-state diffusion, leading to a gradual growth of both grain size and grain number of the decomposition products with increasing milling time.

The second explanation assumes that local melting occurs during impaction of the powder. Several processes should be considered. All intermetallic phases of the Fe–Sn and Co–Sn system melt incongruently and can decompose under high temperature pulses due to ball collisions. After the collision the temperature of the melted regions decreases rapidly and reverse processes of intermetallic formation become possible. All these process must reach a steady state after some time. As a result, the product of MM of FeSn must contain all the phases existing in the Fe–Sn system. The amount of different phases may vary considerably, and only some of them may be detected in the experiment. The value and duration of the local temperature pulses depend mostly on the mechanical parameters of the milling balls, i.e. their sizes, velocity and so forth (see Ref. [13]) for details) and should change only slightly with milling time. Therefore, if decomposition of FeSn and CoSn occurs due to incongruent melting during impaction of the powder, grain sizes of the decomposition products would remain approximately constant during the milling process. Just such a behavior was observed in the present investigations. Using 10^{-7} to 10^{-5} s for the ball collision time and 10 nm for grain sizes and applying the well-known relation $x^2 = 2Dt$, it is possible to estimate for example the diffusion coefficient for growth of Fe_5Sn_3 during powder impaction as $D \approx 5 \times 10^{-6}$ to 10^{-4} cm^2 s^{-1}. This value is also typical of diffusion in a liquid state. Thus, the results obtained in this work support the assumption that local melting is possible during MM process.

While the FeSn and CoSn intermetallics decompose to a large extent upon MM, $CoIn_2$ turns out to be stable, although its melting temperature under normal pressure is essentially lower than that of CoSn. Such observations seem to be in contradiction with a model of local melting but may be explained as follows. As ball collisions generate not only a high local temperature but also a high local pressure, it is reasonable to expect that decomposition is favored if it leads to a decrease in volume. Dachille and Roy [14] reported transformation of solids into denser high-pressure polymorphs due to MM as early as 1960. Yao et al. [15] and Liu et al. [16] have recently shown that an amorphous Fe–N alloy crystallized with formation of the dense high-pressure ε-Fe_xN phase during MM in a vibrating ball-mill. The local pressure was estimated to be in the range from 3.5 GPa to 6.0 GPa and the local temperature to be from 650 K to 1750 K [16].

Calculating volume changes associated with the decomposition of FeSn and CoSn intermetallics into their product phases yield negative values of -0.09 cm^3 and -0.06 cm^3, respectively (for a sample mass of 10 g). In contrast, a decomposition of $CoIn_2$ into the possible product phases, Co and $CoIn_3$, would result in a positive volume change, as $CoIn_2$ has the highest density of all phases in the Co–In system. This is in good agreement with the experimental observations that $CoIn_2$ stays stable during MM. Stresses under ball collisions may well inhibit the decomposition of $CoIn_2$ into a compound of new phases with a lower density.

4. Conclusion

Upon high-energy ball-milling FeSn decomposes into Fe_5Sn_3 and Fe_3Sn_2, while CoSn decomposes into Co_3Sn_2 and Sn(Co). The resulting product phases have the highest densities in the corresponding systems. According to the results of X-ray and magnetization measurements, the grain sizes of the product phases remain approximately unchanged during the milling process. The experimental results on FeSn and CoSn suggest that local melting of powder particles may well take place during high-energy ball-milling in an AGO-2 mill. Although $CoIn_2$ has a lower peritectic melting point than CoSn, no decomposition was detected. Such observations appear to be in contradiction with a model of local melting but can be explained if not only high local temperatures but also high stresses under ball collisions are taken into account.

Acknowledgements

This work was supported by the 2004 Research Fund of the University of Ulsan and (in part) by the Ministry of Commerce, Industry and Energy (MOCIE) of the Republic of Korea, through the Research Center for Machine Parts and Materials Processing (ReMM) at the University of Ulsan.

References

[1] P.I. Loeff, H. Bakker, Europhys. Lett. 35 (1989) 8.
[2] H. Bakker, G.F. Zhou, H. Yang, Prog. Mater. Sci. 39 (1995) 159.
[3] T. Alonso, H. Yang, Y. Liu, P.G. McCormick, Appl. Phys. Lett. 60 (1992) 833.
[4] P.A.I. Smith, P.G. McCormick, Scr. Met. Mater. 26 (1992) 485.
[5] S.L. Tang, C.H. Wu, B.W. Wang, X.V. Jin, G.S. Li, B.Z. Ding, Y.C. Chuang, J. Magn. Magn. Mater. 188 (1998) 387.
[6] S.L. Tang, Z.Q. Jin, S.Y. Zhang, Y.W. Du, Nanostruct. Mater. 12 (1999) 705.
[7] Y.S. Kwon, K.B. Gerasimov, O.I. Lomovsky, S.V. Pavlov, J. Alloys Compd. 353 (2003) 194.
[8] P. Allia, M. Knobel, P. Tiberto, F. Vinai, Phys. Rev. B 52 (1995) 15398.
[9] E. Agostinelli, P. Allia, R. Caciuffo, D. Fiorani, D. Rinaldi, A.M. Testa, P. Tiberto, F. Vinai, Mater. Sci. Forum 235–238 (1997) 705.
[10] F. Vinai, P. Tiberto, A. Deriu, F. Malizia, M. Vittori-Antisari, M. Angliolini, J.S. Pedersen, Mater. Sci. Forum 269–272 (1998) 339.
[11] G. Trumpy, E. Both, C. Diega-Mariadassou, P. Lecocq, Phys. Rev. B 2 (1970) 3477.
[12] T.B. Massalski, Binary Alloy Phase Diagrams, second ed., pASM International, Materials Park, 1990.
[13] D.R. Maurice, T.H. Courtney, Metall. Trans. 21A (1995) 124.
[14] F. Dachille, R. Roy, Nature 186 (1960) 89.
[15] B. Yao, L. Liu, S.E. Liu, B.Z. Ding, W.H. Su, Y. Li, J. Non-Cryst. Solids 277 (2000) 91.
[16] L. Liu, S. Lun, X.D. Zhao, B. Yao, W.H. Su, J. Alloys Compd. 333 (2002) 202.